

The Effect of Rotor Geometry on Particle Size Characteristics for Knife-milled Wheat Straw

Lukáš Krátký^{a,*}, Carlos Arce^a, Tamara Llano^b, Martin Dostál^a, Tomáš Jirout^a

^a Czech Technical University in Prague, Faculty of Mechanical Engineering, Department of Process Engineering, Technická 4, Prague 6, Czech Republic.

^b Green Engineering and Resources Group, Department of Chemistry and Process & Resources Engineering, University of Cantabria, Av. Los Castros 46, 39005, Santander, Spain.
 Lukas.Kratky@fs.cvut.cz

The paper aimed to experimentally identify the effect of rotor blade geometry on particle size characteristics for the knife-milled wheat straw of 12.5 wt % moisture content. Biomass was systematically reduced in size using two-blade rotor geometries (linear and screw), varying the following conditions: rotor speeds of 10.2 - 20.4 m s⁻¹ and screen sieve sizes of 0.75 - 10 mm. It was identified that rotor blade geometry affected particle size. The higher the rotational rotor speed and the screen sieve size, the higher the difference in particle size characteristics. The original empiric model was derived and calibrated by studying the mutual relationships among process variables. The model allows predicting characteristic particle size D_{50} for individual rotor blade geometries, knowing rotor speed and screen sieve size. The accuracies of $R^2 = 0.94$ for linear- and $R^2 = 0.92$ for screw-blade rotor geometry were reached for particle size estimation using the derived model.

1. Introduction

Pretreatment of biomass is a crucial step for lignocellulosic biorefineries. Among them, mechanical size reduction is usually performed. Since it increases specific particle surface area, a critical parameter for intensity transfer phenomena of subsequent biochemical and thermochemical processing steps (Pintana et al., 2020). Kratky and Jirout (2011) reviewed that knife mill belongs to the least energy-demanding group of machines for size reduction of lignocellulosic biomass. The particle size of knife-milled biomass is affected by biomass properties (moisture, total/organic solid content, elementary composition, matrix structure, shear stress, Young modulus) and by the technical set-up of the knife mill (blade geometry, number of static-rotor pairs of blades, rotor revolutions, screen sieve size, mass flowrate).

Conventional knife mills usually use linear, screw or delta rotor blade geometries. Nevertheless, available literature currently provides a tiny amount of information about the effect of rotor blade geometry on particle size and shape for knife-milled biomass. The particle size characteristics are presented for various biomass disintegrated by knife mill equipped with linear rotor blade geometry under varieties in process configurations (biomass type and moisture, number of stator-rotor blade pairs, rotor revolutions, screen sieve size, biomass flowrate) for wheat straw (Bitra et al., 2011), switchgrass and energy cane (Miao et al., 2011), sunflower husks and wood chip pellets (Williams et al., 2017), steam exploded Sakura chips (Priyanto et al., 2017), oak and spruce chips (Eisenlauer and Teipel, 2021), beech chips (Kratky et al., 2021), corn stover and pine chips (Williams et al., 2022). Only Wilcinski et al. (2018) present particle size characteristics for wheat straw reduced in size by a knife mill equipped with a rotor of variant back-rake and blade angles.

The discussed papers applied a knife mill with a linear blade rotor to comminute biomass. No studies were found that analysed the effect of rotor blade geometry on biomass particle characteristics. The paper experimentally assesses the impact of linear- and screw-rotor blade geometry on particle size characteristics for knife-milled wheat straw. It is supposed that screw rotor blade geometry serves coarse particle sizes compared to linear-based ones due to the sequential cutting of biomass by individual screw segments under identical peripheral rotor speeds. The paper aims to confirm or disprove this hypothesis, to derive and calibrate the novel model that allows predicting characteristic particle size knowing rotor geometry, rotor speed and screen sieve size.

2. Material and Methods

All the experimental works were done according to the following systematic procedure.

2.1 Biomass characterization

The wheat straw used to carry out all the experiments evinced moisture content of 12.5 ± 0.06 wt %, total solids of 87.5 ± 0.06 wt % dry mass, and volatile solids of 90.9 ± 0.90 wt % dry mass. The total solids were identified by drying the samples in the dryer (KBC-25W) under 105 °C up to constant weight. The volatile solids were determined by burning the samples in the furnace (LE09/11) under the temperature of 550 °C up to stable weight. Firstly, the knife mill SM300 reduced the raw wheat straw to reach the uniform particle size distribution of the initial sample. The knife mill was equipped with a rotor of linear bladed shape running with a rotational speed of 3000 rpm and a screen sieve of 10 mm in a square opening.

2.2 Experimental set-up

All the experiments were carried out with the knife mill SM300 that was incorporated into the technological set, see Figure 1. First, the raw material is dosed into the mill's hopper, which falls into the mill's size reduction chamber. Manual biomass dosing into the mill was used at the level to keep constant active power during biomass milling and to avoid clogging of the size reduction chamber by biomass. Thus, the stand was equipped with a suction system to enhance the efficiency of fine particle removal out of the size reduction chamber. The systematic experiments were performed considering varieties in rotor blade geometry (linear, screw) as presented in Figure 2, rotor speeds of 10.2 m s⁻¹ (1500 rpm) and 20.4 m s⁻¹ (3000 rpm) and screen sieve with square openings (6 mm, 4 mm, 2 mm) and with trapezoidal ones (1 mm, 0.75 mm), all as independent variables.

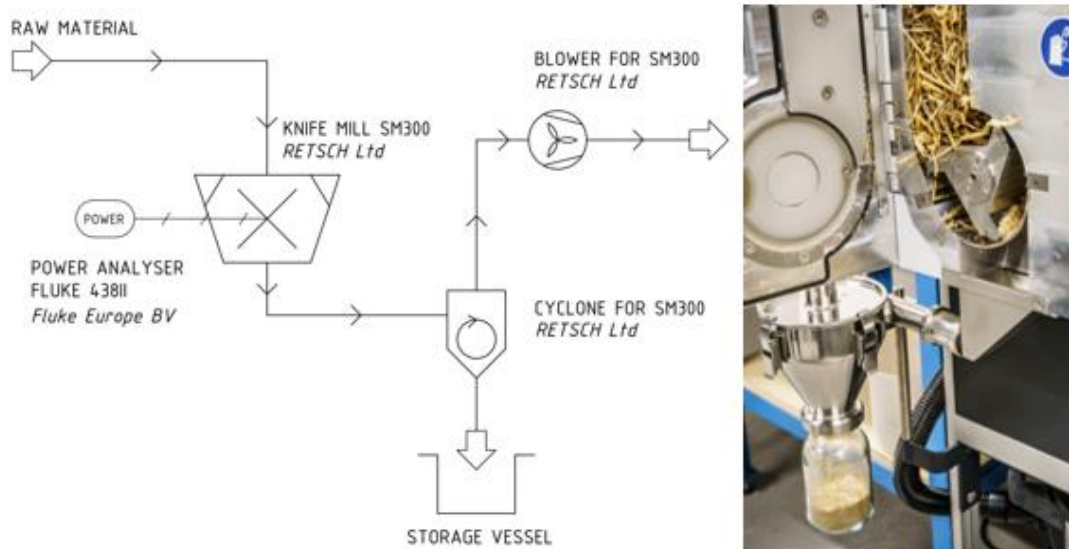


Figure 1: The experimental configuration of the knife mill SM300.

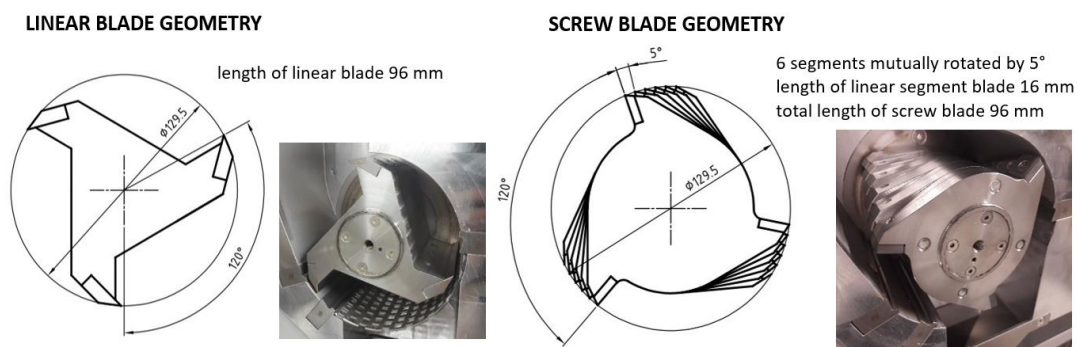


Figure 2: The technical configuration of the experimental equipment.

2.3 Data analysis

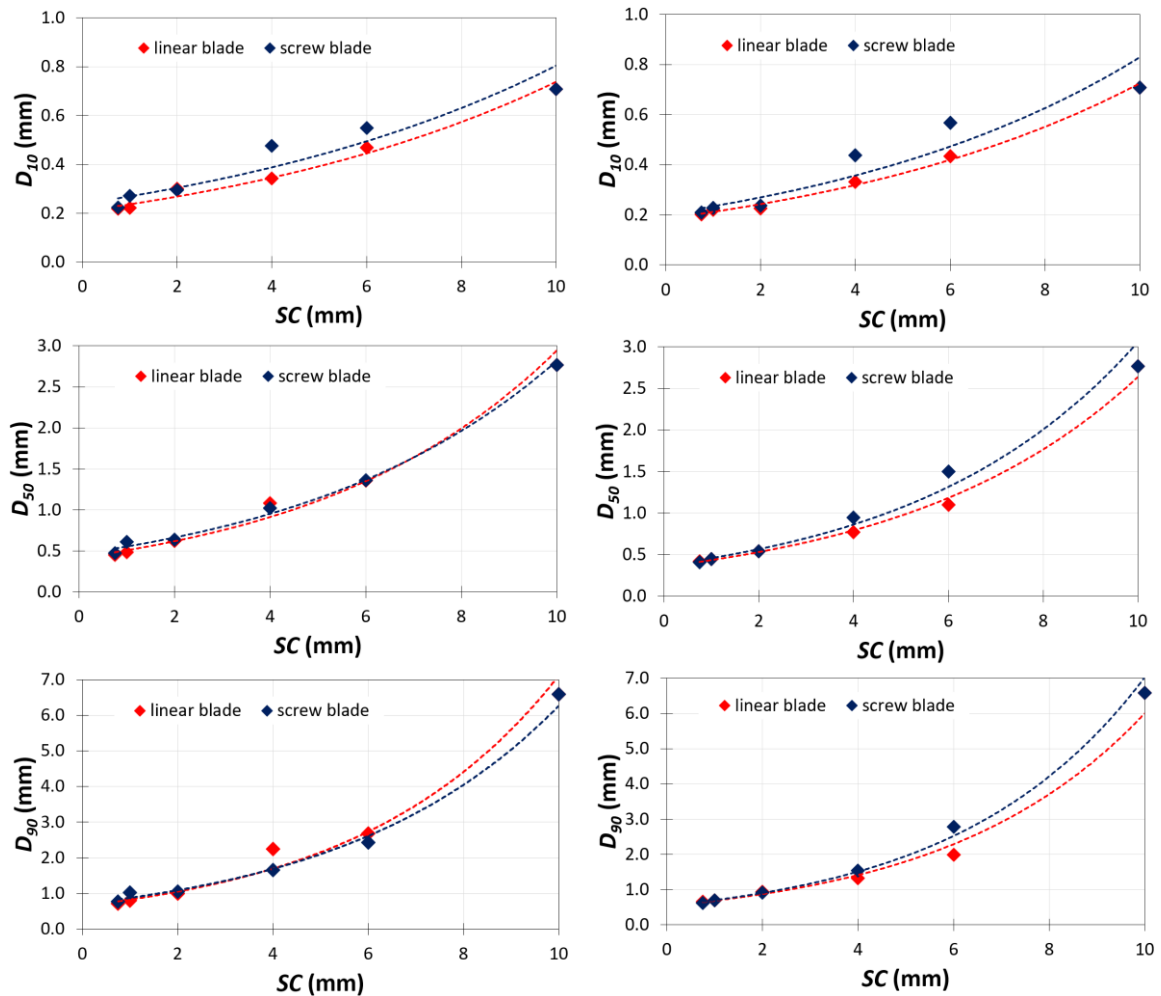
The total mass of the samples and cumulative particle size distribution curves were identified for individual experimental runs for input and output biomass samples. Screen sieve analysis was applied according to ASABE standard S424.1 (2017). In addition, the Rosin-Rammler-Sperling-Bennet (RRSB) model was used to describe the particle size distribution for each comminuted sample, as given by Eq(1). Its polydispersity index n (-) and characteristic particle size D_P (mm) at the cumulative mass fraction 63.2 wt % were identified. Finally, each experimental run was characterized by D_{10} , D_{50} and D_{90} (mm) characteristic particle sizes at the 10th, 50th, and 90th percentiles of cumulative mass distribution and by mass relative span RS_M (-) as a dimensionless measure of particle size distribution width, as defined by Eq(2).

$$F = 1 - e^{-\left(\frac{D}{D_P}\right)^n} \quad (1)$$

$$RS_M = \frac{D_{90} - D_{10}}{D_{50}} \quad (2)$$

3. Results and Discussion

The process characteristics D_{10} , D_{50} , D_{90} and RS_M of individual experimental runs were plotted in dependence on rotor blade geometry, screen sieve size SC and rotor speed v , as plotted in Figure 3 and Figure 4.



A) The rotor speed $v = 10.2 \text{ m s}^{-1}$.

B) The rotor speed $v = 20.4 \text{ m s}^{-1}$.

Figure 3: The comparison of characteristic particle sizes in dependence on process variables (the lines show only the trends).

It was observed that characteristic particle size is slightly affected by rotor blade geometry, as evident from Figure 3. It seems that the higher the rotational rotor speed v and the higher the screen sieve size SC , the higher the difference in particle size characteristics between linear and screw blade rotor geometries. At the same conditions, linear rotor blade geometry tends to generate smaller particle sizes of D_{10} , D_{50} , and D_{90} than screw rotor blade shapes. These results endorse the hypothesis that screw rotor blade geometry serves coarse particle sizes compared to linear-based ones due to the sequential cutting of biomass by individual screw segments. The higher the rotor speed, the lower particle size characteristic both for linear and screw rotor blade geometries. Similar particle size characteristics were reported for wheat straw (Bitra et al., 2011) and wooden chips (Kratky et al., 2021), all knife-milled with the rotor having linear blade geometry. Moreover, the screw blade geometry provides lower mass relative span RS_M values, as plotted in Figure 4. It means that lower dimensionless particle size distribution width was reached for screw blade geometry compared to a linear one at the rotor speed of 10.2 m s^{-1} . On the contrary, there is no evident difference between the RS_M values of both blade geometries at a rotor speed of 20.4 m s^{-1} . This means that the lower the rotor speeds, the broader the particle size distribution for linear blade geometry to screw one.

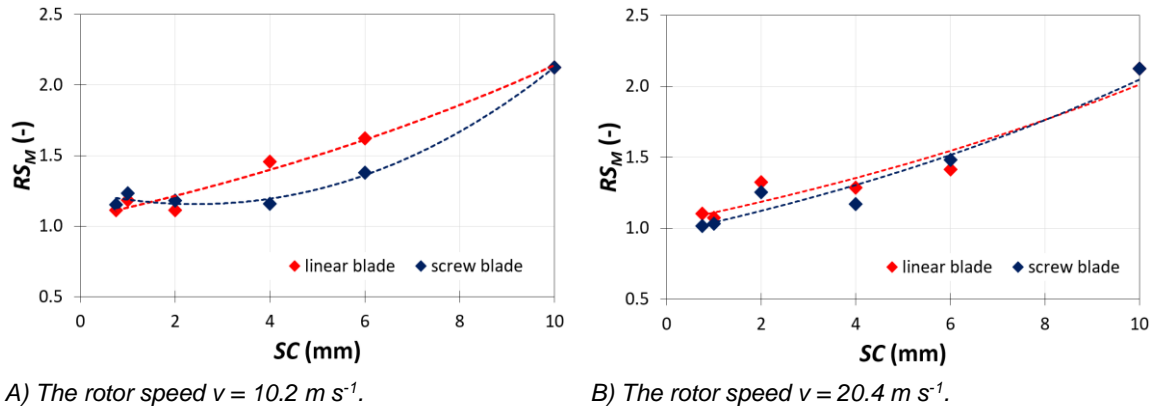


Figure 4: The comparison of RS_M in dependence on process variables (the lines show only the trends).

Each experimental run was characterised by cumulative particle size distribution curves described by the RRSB model. Knowing its characteristic particle size D_P and polydispersity index n , allows calculating a characteristic particle size D_F at a given cumulative mass fraction F according to Eq(3).

$$D_F = D_P \cdot [-\ln(1 - F)]^{1/n} \quad (3)$$

The particle size D_{50} at the cumulative mass fraction of 50 wt % is usually served as the representative particle size of the comminuted sample as presented for wheat straw (Bitra et al., 2011), oak and spruce wood chips (Eisenlauer and Teipel, 2021), switchgrass (Miao et al., 2011), sunflower husks and wood chip pellets (Williams et al., 2017). Setting $F = 0.5$, $D_F = D_{50}$ in Eq(3), the D_{50} particle size is defined as follows.

$$D_{50} = D_P \cdot e^{-\frac{0.366513}{n}} \quad (4)$$

$$D_P = A \cdot e^{B \cdot SC} = (a \cdot v) \cdot e^{(b \cdot v) \cdot SC} \quad (5)$$

$$n = C \cdot SC + D = (c \cdot v) \cdot SC + (d \cdot v) \quad (6)$$

Eq(4) predicts characteristic particle sizes by knowing the dependences of D_P and n on rotor geometry, screen sieve size SC and rotor speed v . The D_P value evinced the exponential dependence on screen sieve size for both geometries, as plotted in Figure 4. The physical explanation of this dependence is as follows. Regarding one pair of stator-rotor blades, one cut creates two particles of the initial one. Two cuts generate four particles. Three cuts form up to eight particles. It means that the particle quantity exponentially depends on the number of cuts in horizontal, vertical and diagonal directions. Moreover, similar trends were reported for oak and spruce wood chips (Eisenlauer and Teipel, 2021) and wheat straw (Kratky et al., 2021). Thus, the dependence of RRSB particle size D_P on screen sieve size SC can be empirically modelled by Eq(5), in which a and b are regressed

parameters. The exponential function coefficients, i.e. A and B , depend on rotor speed v . The approximative linear dependence of A and B parameters on rotor speed v was assumed due to the proximities of the curves for individual rotor speeds.

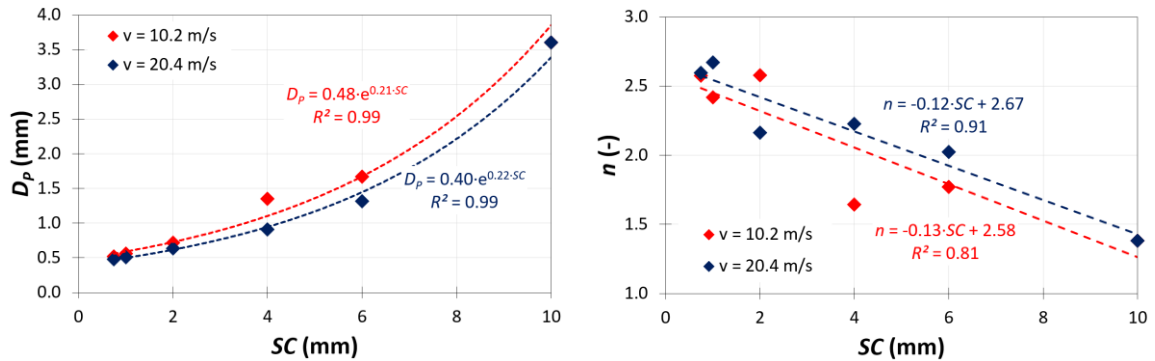


Figure 5: The linear blade geometry - the characteristics of the RRSB model (D_p , n) concerning SC and v .

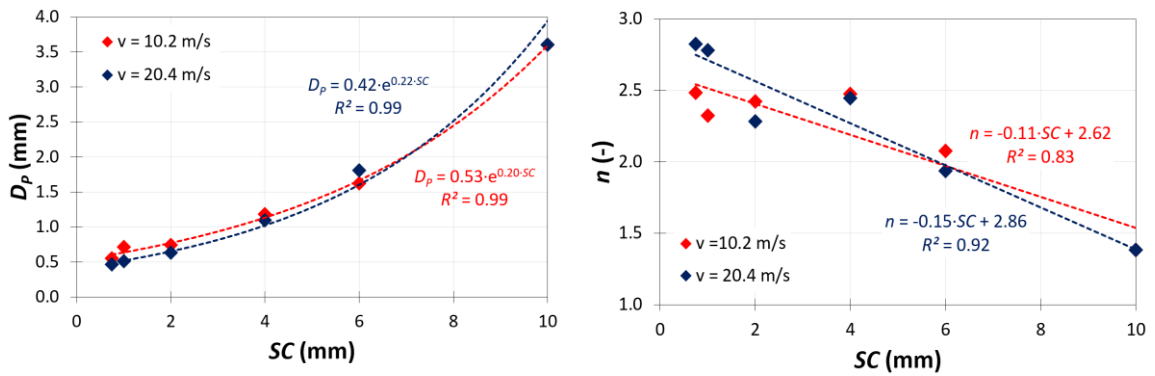
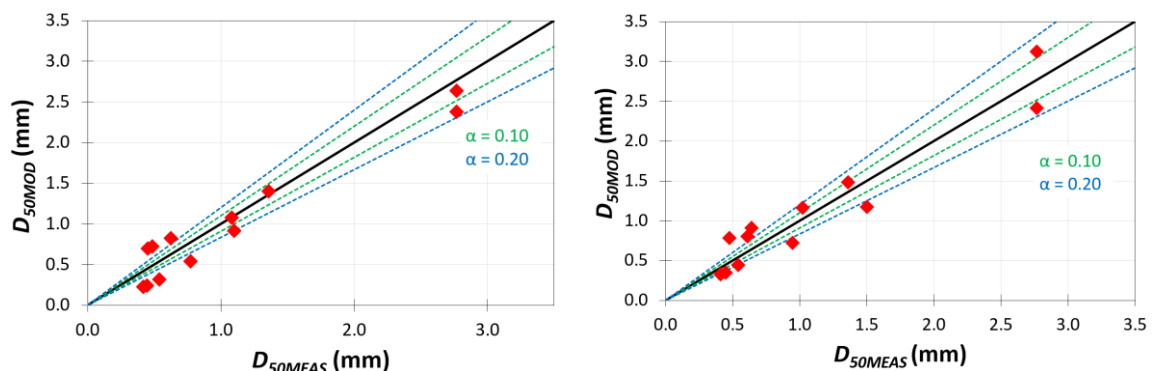


Figure 6: The screw blade geometry - the characteristics of the RRSB model (D_p , n) concerning SC and v

The linear relationship between polydispersity index n and screen sieve size SC was identified as presented in Figure 5 and Figure 6 for both blade geometries. The lower the screen sieve size SC , the lower the heterogeneity of a sample, expressed as the increase in the polydispersity index n . Thus, the dependence of polydispersity index n on screen sieve size SC shows linear dependence as defined by Eq(6), in which c and d are regressed parameters. Both coefficients of the linear function, i.e. C and D , depend on rotor speed v . The approximative linear dependence of C and D parameters on rotor speed v was assumed due to the proximities of the curves for individual rotor speeds.



A) The linear blade geometry.

B) The screw blade geometry.

Figure 7: The comparison of measured D_{50MEAS} and predicted D_{50MOD} values according to Eq(7) equipped with the confidence intervals defined by a value.

Inserting Eq(5) and Eq(6) into Eq(4), the general empiric model is defined by Eq(7) that allows predicting characteristic particle size D_{50} for individual rotor blade geometries, knowing rotor speed v (m s^{-1}) and screen sieve size SC (mm).

$$D_{50} = a_1 \cdot v \cdot e^{(a_2 \cdot v \cdot SC + a_3 \cdot v)} \quad (7)$$

The coefficients of a_1 , a_2 , a_3 were reached by Matlab's nonlinear regression of Eq(7) to experimental identified D_{50} values for individual geometries. The values $a_1 = 0.422 \pm 0.123$, $a_2 = 0.013 \pm 0.002$, and $a_3 = -0.188 \pm 0.032$ were found for linear blade rotor geometry. The values $a_1 = 0.368 \pm 0.127$, $a_2 = 0.012 \pm 0.003$, and $a_3 = -0.163 \pm 0.034$ were found for screw blade rotor geometry. The model and its coefficients of a_1 , a_2 , and a_3 are valid for knife milling of wheat straw with the moisture of 12.5 wt %, rotor speed of 10.2-20.4 ms^{-1} , screen sieve sizes of 0.75-10.00 mm and biomass flowrate of 51-112 $\text{kg h}^{-1} \text{m}^{-1}$ related to length of size reduction zone. The accuracies of $R^2 = 0.94$ for linear- and $R^2 = 0.92$ for screw-blade rotor geometry were reached for particle size estimation using the derived model. Finally, the plots of D_{50} measured D_{50MEAS} and predicted by model D_{50MOD} were compared in Figure 5. The general confidence intervals α of 10 % and 20 % were plotted for the diagonal linear curve in the Figure. The closest points to the diagonal, the better precision is reached. Regarding the Figure, it can be concluded that most data is located in the confidence level of $\alpha = 0.20$.

4. Conclusions

This experimental study confirmed the assumption that particle size is affected by rotor blade geometry. The higher the rotational rotor speed and the higher the screen sieve size, the higher difference in particle size characteristics between linear and screw blade rotor geometries. The higher the rotor speed, the lower particle size characteristic both for linear and screw rotor blade geometries. The research needs and challenges are viewed in profound studies on how blade shape geometry affects biomass particle size and shape. Finally, using the RRSB model as a base, the original empiric model was derived and calibrated. The model allows predicting characteristic particle size D_{50} for individual rotor blade geometries, knowing rotor speed and screen sieve size.

Acknowledgments

This research was supported by the Ministry of Education, Youth and Sports of the Czech Republic under OP RDE grant number CZ.02.1.01/0.0/0.0/16_019/0000753 "Research centre for low-carbon energy technologies".

References

- ASABE S424.1, 2017, Method of determining and expressing particle size of chopped forage materials by screening, American Society of Agricultural and Biological Engineers, St. Joseph, USA.
- Bitra V.S.P., Womac, A.R., Yang Y.T., Miu P.I., Igathinathane C., Chevanan N., Sokhansaj S., 2011, Characterization of wheat straw particle size distributions as affected by knife mill operating factors, *Biomass and Bioenergy*, 35, 3674-3686.
- Eisenlauer M., Teipel U., 2021, Comminution energy and particulate properties of cutting and hammer-milled beech, oak, and spruce wood, *Powder Technology*, 394, 685-704.
- Kratky L., Jirout T., 2011, Biomass size reduction machines for enhancing biogas production, *Chemical Engineering and Technology*, 34, 391-399.
- Kratky L., Jirout T., 2020, Modelling of particle size characteristics and specific energy demand for mechanical size reduction of wheat straw by knife mill, *Biosystems Engineering*, 197, 32-44.
- Kratky L., Jirout T., Dostal M., Ayas M., 2021, The effect of moisture on the particle size characteristics of knife-milled beech chips, *Chemical Engineering Transactions*, 88, 739-744.
- Miao Z., Grift T.E., Hansen A.C., Ting K.C., 2011, Energy requirement for comminution of biomass in relation to particle physical properties, *Industrial Crops and Products*, 33, 504-513.
- Pintana P., Thanompongchart P., Dussadee N., Tippayawong N., 2020, Overview of palletisation technology and pellet characteristics from maize residues, *Chemical Engineering Transactions*, 78, 121-126.
- Priyanto D.E., Ueno S., Hashida K., Kasai H., 2017, Energy-efficient milling method for woody biomass, *Advanced Power Technology*, 28, 1660-1667.
- Wilczyński D., Talaśka K., Malujda I., Jankowiak P., 2018, Experimental research on biomass cutting process, *MATEC Web of Conferences*, 157, 07016.
- Williams L., Karlsson M.C.F., Emerson R.M., Smith W.A., Bhattacharjee T., 2022, Green biomass processing to lower slurry viscosity and reduce biofuel cost, *Biomass and Bioenergy*, 165, 106566.
- Williams O., Lester E., Kingman S., Giddings D., Lormor S., Eastwick C., 2017, Benefits of dry comminution of biomass pellets in a knife mill, *Biosystems Engineering*, 160, 42-54.